ACI STRUCTURAL JOURNAL TECHNICAL PAPER

Title no. 97-S12

Analysis of Shear-Critical Reinforced Concrete Beams

by Frank J. Vecchio

Recent experience among some researchers suggests that analysis methods based on the smeared rotating crack concept do not adequately model the response of shear-critical concrete beams containing little or no shear reinforcement. Application of the modified compression field theory (MCFT), one of the first such rotating crack models, to the analysis of shear beams is addressed herein. The original constitutive relations are re-examined, and a crack width limit and residual tension term are introduced. When incorporated into a nonlinear finite element procedure, the model is shown to adequately simulate the strength, stiffness, ductility, and failure mode of lightly reinforced shear-critical test beams. Sectional analysis procedures based on the same model are also shown to provide accurate predictions of response. Prevailing mechanisms are discussed, and aspects of the model in need of further refinement are also identified.

Keywords: beams (supports); concretes; cracking (fracturing); shear properties; tension; tests.

INTRODUCTION

The behavior and design of reinforced concrete beams in shear remains an area of much concern. Approximately 40 years after the collapse of the U.S. Air Force hangars, attributed to inadequate shear design practice, research activity in this area continues. Design code procedures are continually changing and generally becoming more stringent. Structures that were designed several decades ago typically do not comply with the requirements of current codes, with the implication that massive amounts of funds must be spent on rehabilitating or upgrading the infrastructure. It remains a pressing need to establish design and analysis methods that provide realistic assessments of the strength, stiffness, and ductility of shear-critical elements.

Among the theoretical formulations developed in recent years for this purpose was the modified compression field theory (MCFT),[1] essentially a smeared, rotating crack model for cracked reinforced concrete elements. On the basis of a number of panel tests, constitutive relations were developed describing the behavior of cracked reinforced concrete in compression and in tension. This behavior, influenced by such mechanisms as compression softening and tension stiffening, is fundamentally different from that of plain concrete. The constitutive models developed were incorporated into new design procedures[2] that form the basis for the general method for shear design in the Canadian Code, CSA A23.3 M94. They were incorporated into the formulation of various nonlinear finite element algorithms as well.[3-5] The resulting analysis procedures have been shown to provide accurate simulations of response for a wide range of structures including beams in flexure, shear and torsion, deep beams, shear walls, columns, and plates and shells.[6]

The use of smeared rotating crack models has gained some degree of acceptance among analysts; thus, several alternative, but essentially similar, formulations were developed by a number of researchers.[7-9] In addition, other researchers opted for smeared, fixed crack models.[10,11] In general, formulations of both types can be shown to provide good correlations with test data for structures that are orthogonally reinforced with the reinforcement ratio in the weaker direction being 0.1% or greater.

According to researchers, however, in the application to beams with little or no shear reinforcement, and loaded so as to be critical in shear, the accuracy of the various analysis procedures has shown some deficiencies. Chung and Ahmad[12] concluded that "results indicate that the MCFT is not applicable to lightly reinforced or unreinforced concrete member." These conclusions, however, were based on analyses that were an incomplete adaptation of the theory (refer to discussions in Reference 13).

Youb and Filippou,[8] using a model that is an extension of both the MCFT and work by Balakrishnan and Murray, were able to get good results for many structure types except lightly reinforced shear beams. Here, "numerical difficulties were, however, encountered when the crack distribution in the structural element does not satisfy the assumptions of the smeared crack model, as in the case of beams without shear reinforcement." Hsu and Zhang[14] also encountered problems in applying their rotating crack model to elements lightly reinforced in one direction. This prompted them to propose a fixed-crack model for use in such situations. On the other hand, Foster,[9] among others, reported good success in using rotating crack models in the analysis of shear critical beams.

Most smeared, rotating crack models are based on formulations involving average strains and average stresses. Few give consideration to local stress conditions at crack locations, although some (for example, Maekawa[10]) incorporate a crack slip check. In the analysis of adequately reinforced structures, the resulting cracks are well distributed and the analyses typically provide accurate simulations. In lightly reinforced shear beams, however, behavior is often governed by the formation of a dominant shear crack. Here, a consideration of the local stress conditions adjacent to the crack is critical to a proper analysis, hence the difficulty encountered by some of the previously cited researchers and others.

RESEARCH CONTRIBUTION

This paper will address the applicability and accuracy of smeared, rotating crack models to the analysis of shear-critical beams. In particular, it will focus on the aspects of the formulations that can potentially corrupt accuracy and identify some minor additions to the formulation that improve results. It will show, contrary to the conclusions of some other researchers, that rotating crack analyses can provide an accurate representation of the strength, stiffness, and ductility of lightly reinforced shear-critical beams.

CONSTITUTIVE MODELING

The modified compression field theory is a smeared, rotating crack model for simulating reinforced concrete behavior. Cracked concrete is treated as an orthotropic material with unique stress-strain characteristics that are, to some extent,

ACI Structural Journal, V. 97, No. 1, January-February 2000.
Received September 23, 1998, and reviewed under Institute publication policies.

Frank J. Vecchio, *FACI, is Professor of Civil Engineering at the University of Toronto, Ontario, Canada. He is a member of Joint ACI-ASCE Committees 441, Reinforced Concrete Columns; and 447, Finite Element Analysis of Reinforced Concrete Structures. His research interests include constitutive modeling of reinforced concrete, development of nonlinear analysis procedures, and repair and rehabilitation of concrete structures.*

dependent on the amounts of reinforcement present. For the composite element, composed of concrete and any number of reinforcement components of arbitrary direction, equations of equilibrium, compatibility, and constitutive response are developed. These equations are formulated in terms of average stresses and average strains in the materials. A key aspect of the model, however, is to also examine and satisfy local stress conditions at crack locations. Another key assumption of the theory is that the directions of principal strain in the concrete coincide with the directions of principal stress under monotonic loading conditions. The formulations of the MCFT are documented elsewhere;[1,15] herein, it will be useful to review the constitutive modeling of the concrete.

The strength and stiffness of concrete in compression is reduced by the presence of transverse cracking. In a principal compression strain direction, the principal compressive stress f_{c2} is calculated from the corresponding strain ε_2 by the following relationship

$$f_{c2} = -f_p\left[2\left(\frac{\varepsilon_2}{e_p}\right) - \left(\frac{\varepsilon_2}{\varepsilon_p}\right)^2\right] \tag{1}$$

where

$$f_p = \beta_d \cdot f_c' \tag{2}$$

$$\varepsilon_p = \beta_d \cdot \varepsilon_o \tag{3}$$

$$\beta_d = \frac{1}{0.35\left(-\frac{\varepsilon_1}{\varepsilon_2} - 0.28\right)^{0.8}} \leq 1.0 \tag{4}$$

Note that the damage factor β_d is a function of the principal tensile strain ε_1 in the direction normal to the compression direction. A more complete discussion of this so-called compression softening effect is given in Reference 16.

For concrete in a principal tensile strain direction, prior to cracking, a linear relation is used. Thus, the principal tensile stress f_{c1} is

$$f_{c1} = E_c \cdot \varepsilon_1 \tag{5}$$

where E_c is the initial tangent modulus of the concrete. After cracking, the following relation is employed to reflect tension stiffening effects

$$f_{c1} = \frac{f_t'}{1 + \sqrt{500 \cdot \varepsilon_1}} \tag{6}$$

where f_t' is the tensile cracking strength.

It is important, particularly in concrete beam elements containing little or no shear reinforcement, to check that the concrete tensile stresses can be transmitted across cracks. For an element containing n number of reinforcement components, the local crack check is

$$f_{c1} \leq \sum_{i=1}^{n} \rho_i (f_{yi} - f_{si}) \cdot \cos^2\theta_{ni} \tag{7}$$

where ρ_i is the reinforcement ratio, f_{yi} is the yield stress, f_{si} is the average stress, and θ_{ni} is the angle between the reinforcement and the normal to the crack. Note that for areas of concrete containing no reinforcement, the implication of Eq. (7) is that no postcracking tensile stress can exist.

To transit the average concrete stresses across the cracks, the local stresses in the reinforcement must be increased at the crack locations. This gives rise to shear stresses on the crack surfaces because the local stress directions no longer coincide with the average principal strain directions. The calculated shear stress on the crack surface v_{ci} is checked against a limiting stress v_{cimax}, which is based on the work of Walraven.[17] Thus

$$v_{cimax} = \frac{0.18\sqrt{f_c'}}{0.31 + \frac{24w}{a + 16}} \tag{8}$$

where w is the crack width and a is the aggregate size. If v_{ci} exceeds v_{cimax}, then it is assumed that slip is occurring on the crack surface and the concrete tensile stress must be reduced. The stress f_{cl} is reduced until $v_{ci} < v_{cimax}$.

The MCFT and the constitutive relationships described previously were incorporated into a number of analysis procedures including various nonlinear finite element routines.[3-5] In applications to a diverse range of concrete structures, the procedure has been shown to provide accurate simulations of behavior. Other researchers, using similar procedures, have also reported good success.

APPLICATION TO SHEAR-CRITICAL BEAMS

The MCFT was based on certain assumptions that bear reexamination in the context of beams containing little or no shear reinforcement. Relevant to this discussion are three basic suppositions:

1. Stresses and strains are treated in terms of average values. This implies formation of a fairly well distributed pattern of cracks, as opposed to a situation where behavior is governed by one or two dominant cracks;

2. Postcracking tensile stresses exist in the concrete as a consequence of tension stiffening mechanisms between the reinforcement and the concrete; and

3. Principal strain directions are coincident with principal stress directions.

Consider a concrete beam containing a low amount of transverse reinforcement, and loaded in a manner to be shear critical (Fig. 1). In such an element, it is typical to see a crack pattern dominated by a few large cracks running from the load application point to the supports. Such cracks can exceed several millimeters in width, while the cracks elsewhere remain of negligible width. A case in point would be Beam WM100D, tested by Collins and Stanik,[18] shown in Fig. 2. At maximum load, the principal shear crack has a width of 6.0 to 7.0 mm; elsewhere, the cracking is minor and limited to widths of 0.1 to 0.2 mm. In such cases, consideration of local stress conditions and the flow of forces across cracks takes on heightened importance. Further, it has been observed in tests of such beams that a measurable amount of slip occurs along the crack. This slip distortion, if not taken into account in the element compatibility relations (MCFT currently does not), results in an apparent violation of the assumption that principal stresses remain aligned with principal strains. Finally, if a finite element (FE) analysis is undertaken for the beam, the elements used to model the web portion of the

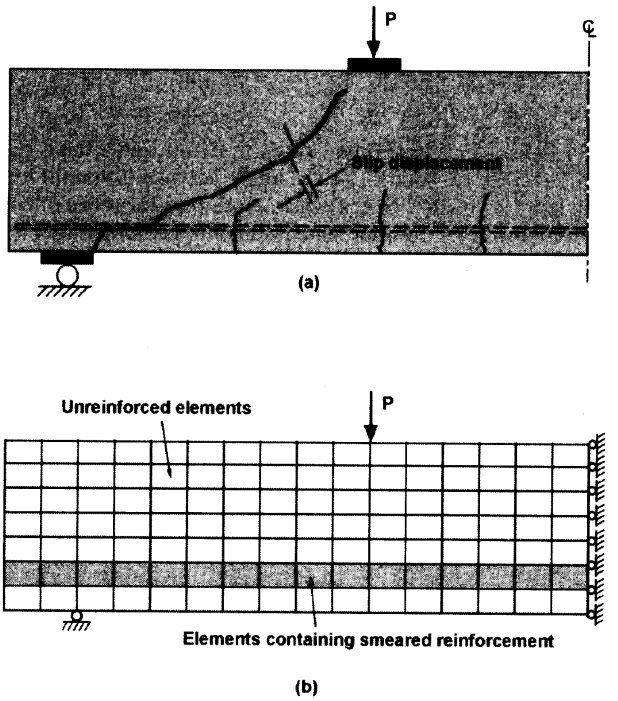

Fig. 1—Typical shear beam; (a) formation of dominant shear crack; and (b) FE representation of beam.

beam will contain no reinforcement. Hence, no postcracking tensile stresses can be sustained in the web owing to Eq. (7). These postcracking tensile stresses, essentially equivalent to the concrete contribution V_c prescribed in the ACI Code and other standards, are necessary to complete the internal truss-like load resisting mechanism. Without them, the beam fails shortly after cracking.

Thus, in applying smeared rotating crack models to the analysis of shear beams, the range of applicability of the formulations is tested. While some researchers have reported good success in modeling shear-critical beams using such models, others have not. Shown in Fig. 3, for example, are analyses for Bresler and Scordelis[19] Beams A-1 and OA-1, determined using the MCFT relationships as originally constituted and previously presented. Beam A-1 contained a relatively low amount of shear reinforcement at 0.10% and sustained a shear failure. The computed strength and load-deformation response are a reasonably accurate approximation to the measured response. Beam OA-1 was similar to Beam A-1 but contained no shear reinforcement. The computed response for Beam OA-1 now shows considerable deviation from the test results. In general, it is found that for shear-critical beams containing light amounts of shear reinforcement, from approximately 0.05 to 0.10%, the strength is underestimated and the ductility overestimated. For shear-critical beams containing no shear reinforcement, strength is typically underestimated by a significant amount.

In shear beams having low shear span-to-depth ratios from approximately 2.0 to 3.0, a counteracting trend can prevail. In the analyses of such beams, the computed rotation of the cracks may proceed to the extent where a large portion of the load is taken to the support by direct strut action. In reality, slip along the cracks can delay or prevent such a reorientation of the stress trajectories. Herein, it is common to see the computed strength and stiffness exceed the measured values by a significant amount.

While a relatively high degree of scatter should be expected for concrete elements strongly influenced by the concrete tensile strength and aggregate interlock, there are other underlying factors for this systematic deterioration in accuracy. These relate back to the three assumptions previously cited, and the formulations that are derived from them. A closer examination follows.

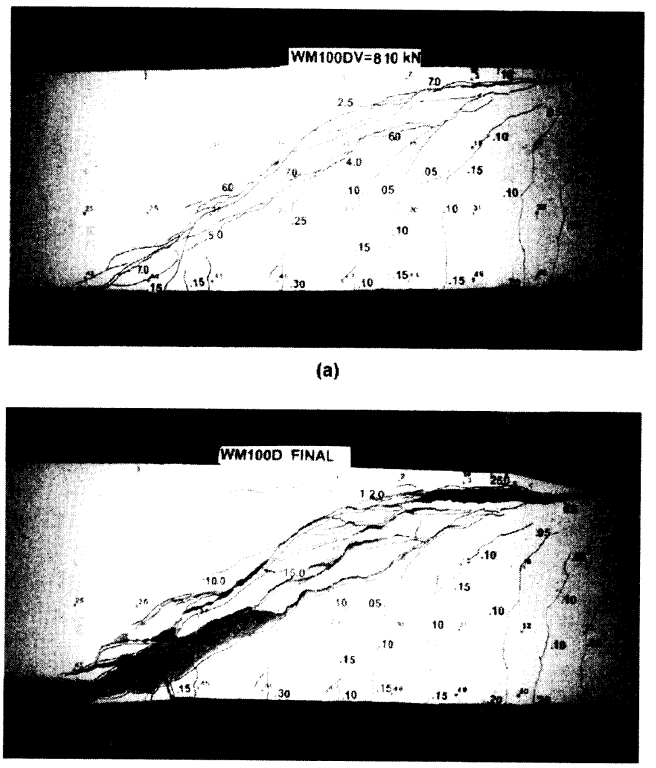

Fig. 2—Beam WM100D tested by Collins and Stanik: (a) at ultimate load; and (b) at failure. (Crack widths shown in mm.)

CRACK WIDTH LIMIT

Perhaps the single most important aspect of the analysis theory, embodied in Eq. (1) through (4), is the premise that the compression strength of concrete is adversely affected by transverse cracking. A re-examination of this compression-softening behavior, conducted more recently[16] using a much larger database, essentially reaffirmed the original findings and produced a slightly modified formulation. It is useful to examine the nature of the data used to formulate the original and updated versions of the compression-softening damage factor β_d. Shown in Fig. 4 are the principal compression stress-strain data obtained from over 200 panel tests conducted over the past 20 years, including several panels that were uniaxially reinforced or contained very light amounts of reinforcement in one direction. The plots indicate that relatively few data were collected for strain conditions where the principal tensile strain exceeded 12×10^{-3} (assume $\varepsilon_0 \approx 2.0 \times 10^{-3}$), or where the ratio of principal strains ($\varepsilon_1/\varepsilon_2$) exceeded 16.

In this context, it is useful to examine more closely the computed response of Beam A-1. At an imposed midspan deflection of 18 mm, near the ultimate load condition, the FE analysis indicates that a large inclined crack had formed in the web region of the beam. The most critically stressed element in the FE analysis, located on this crack plane, is situated at middepth approximately 1000 mm from the support. In this element, the calculated principal tensile strain is 45.0×10^{-3} and the principal compressive strain is -1.48×10^{-3}, giving a $\varepsilon_1/\varepsilon_2$ ratio of 30. Further, the strain conditions result in a computed crack width of 7.2 mm (determined as $w = s \cdot \varepsilon_1$ where s is the average crack spacing). The coexisting principal compressive stress is found to be −3.02 MPa. (Other elements straddling the dominant shear crack exhibit similar states.) Clearly, the strain

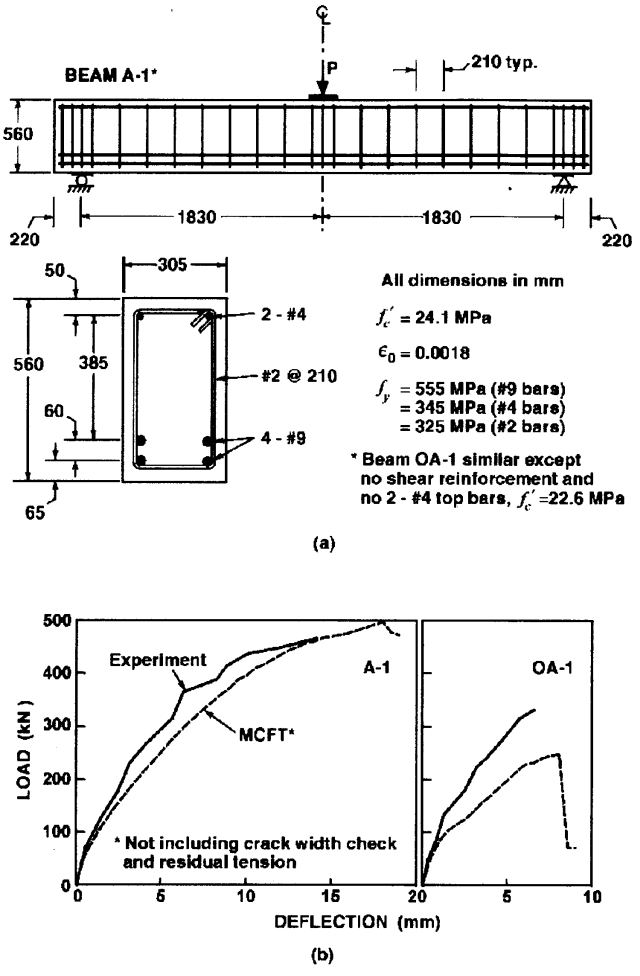

Fig. 3—Bresler-Scordelis Beams A-1 and OA-1: (a) beam details; and; (b) correlation of analysis to measured load-deflection response, assuming original MCFT formulation.

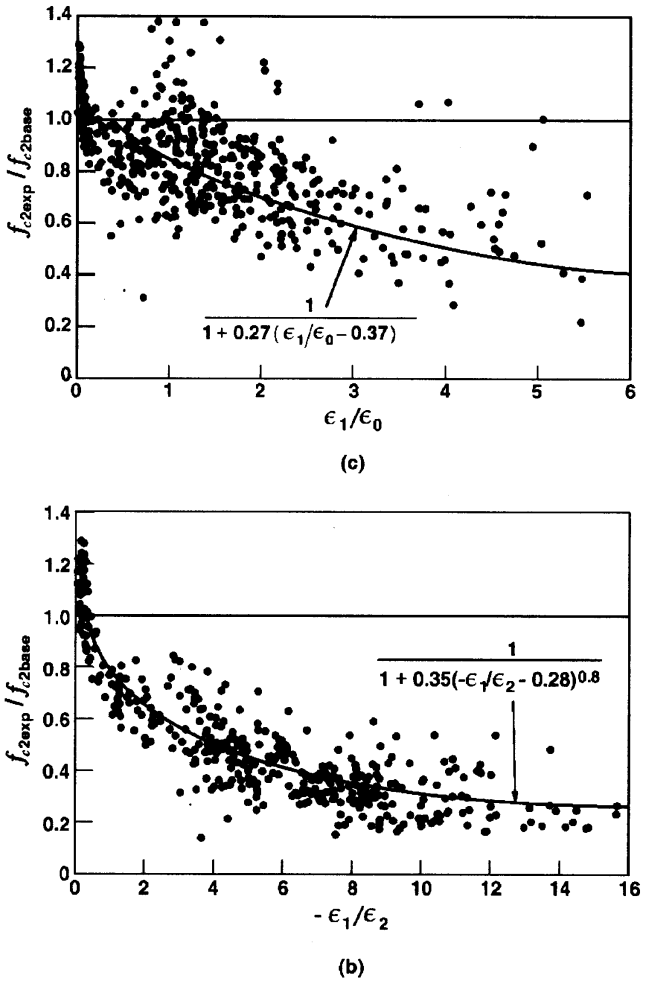

Fig. 4—Compression softening data obtained from panel tests: (a) range of principal tensile strain, ϵ_1; and (b) range of strain ratio $-\epsilon_1/\epsilon_2$.

conditions are well beyond the range for which the compression softening relationships were calibrated.

While the compressive stresses in lightly reinforced shear beams are relatively small (in this case about $0.15f_c'$ and equal to the calculated f_p), small levels of compression are all that is required to transfer the loads via strut action to the supports. As a consequence of slip along the crack surface, however, the orientation of the local stress field may not be coincident with the computed inclination of the average principal strains and average principal stresses. Thus, the compression stresses, albeit small, may be crossing the crack plane. In this case, where the crack is in excess of 7.0 mm wide, such an occurrence is highly unlikely by any means. Thus, an additional condition must be imposed in such anomalous situations to guard against this possibility.

In shear critical beams, it is typically found that the formation of a dominant shear crack is localized in a narrow band of elements. In these elements, it is reasonable to discount completely their ability to sustain compressive stresses. For the analyses reported herein, it was found that imposing a 2 mm crack width limit yields, in most cases, significantly improved results. Thus, in conjunction with the compression softening formulation, it is proposed that when the computed crack width in an element exceeds 2.0 mm, the computed principal compression stress be reduced according to the following relationship

$$f_{c2} = f_{c2}' [5-w/3]; \quad 2 \le w \le 5 \qquad (9a)$$

$$= 0; \quad w > 5 \qquad (9b)$$

where f_{c2}' is the stress computed using Eq. (1) through (4), and w is the crack width.

The principal effect of imposing the crack width limit on the compression softening formulation is to restrict the computed ductility in lightly reinforced shear-critical elements. In most other situations, the crack width limit has little or no influence. As will be shown, the overly ductile computed response for Beam A-1, and similar beams, is largely corrected as a result of this check.

RESIDUAL TENSION

As discussed, in beams containing low amounts of shear reinforcement, the concrete contribution plays a major role in forming a viable internal load resisting mechanism for shear forces. This concrete contribution is derived from mechanisms such as aggregate interlock, dowel action, and the interaction between the concrete and the reinforcement commonly known as tension stiffening. With respect to the latter, it is commonly accepted that the interaction effects are transmitted to a zone of concrete within approximately 7-1/2 bar diameters from the reinforcement or less, as suggested by the CEB-FIP model code.

In the FE modeling of reinforced concrete elements, aggregate interlock and tension stiffening effects can be represented by a formulation allowing for postcracking tensile stresses in the concrete (for example, Eq. (6)). As previously discussed, however, it is necessary to check that these stresses can be transmitted across the crack; hence, the need for Eq. (7). The check is made for each element, according to the stresses and reinforcement conditions in that particular element. The difficulty that

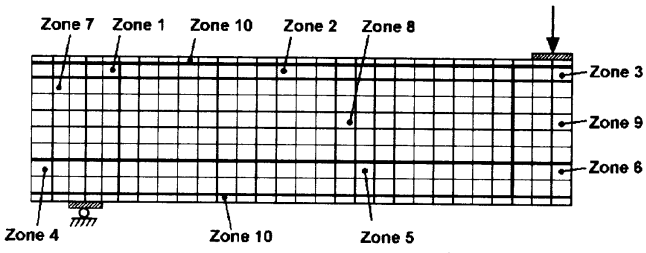

Zone	1	2	3	4	5	6	7	8	9	10
ρ_x (%)	1.626	1.626	1.626	6.816	6.816	6.816	0.000	0.000	0.000	0.000
ρ_y (%)	0.187	0.099	0.282	0.187	0.099	0.282	0.187	0.099	0.282	0.000

Fig. 5—Typical FE mesh used to model Bresler-Scordelis beams. Mesh shown for A-1.

arises is that the tension stiffening action in the actual beam may be induced by reinforcement that is located some distance away. In relation to shear beams, and in Beam OA-1, for example, the bottom reinforcement will give rise to tension stiffening effects throughout much of the tension zone, if one accepts the 7-1/2 bar diameter guideline. Yet it is common to model the reinforcement as discrete bars or as smeared within a narrow band of elements coincident with the centerline of the reinforcement. The elements in the middepth regions of the beam are represented as unreinforced, and hence unable to develop any postcracking tensile stresses owing to the restrictions of Eq. (7). This results in typically underestimated shear capacities for beams containing no shear reinforcement and is largely the result of modeling strategy rather than deficiencies in the constitutive models.

In shear-critical unreinforced elements, it has been found that using a residual concrete tensile stress of 0.10 to 0.15 f'_t for concrete in tension leads to much improved analytical results. (The concrete cracking stress f'_t is taken as $0.33\sqrt{f'_c}$.) Foster[9] has done essentially the same, using a lower limit of 0.30 to 0.40 f'_t on the postcracking tension curve. He also reported good correlation with test data. Thus, for unreinforced elements exposed to high transverse shear conditions, it is proposed that

$$f_{c1} \geq 0.10 f'_c \qquad (10)$$

The effect of including this lower limit on the tension stiffening stresses is to improve strength predictions in beams having low shear reinforcement ratios ρ_v of less than approximately 0.05%. As ρ_v values increase beyond that level, the influence quickly diminishes (a residual tension should not be used in elements primarily experiencing membrane tension stresses, as in the flanges of beams or shear walls; it can lead to overestimated tension forces capacities).

It is interesting to note that in fixed crack models, a shear retention factor β is commonly used to relate the ratio of the postcracking shear stiffness in the concrete to the precracking stiffness. It essentially serves the same purpose as the residual tension term proposed previously; that is, to ascribe some tensile strength and stiffness to the unreinforced concrete even through it is cracked and presumably incapable of resisting diagonal tension. While a large range of values has been reportedly used for this factor, it also is commonly taken to be approximately 0.05 to 0.10.

CORROBORATION WITH TEST BEAMS

The series of beams tested by Bresler and Scordelis,[18] owing to the high quality of the testing and the results, is often used for benchmark purposes. The beams were designed and loaded

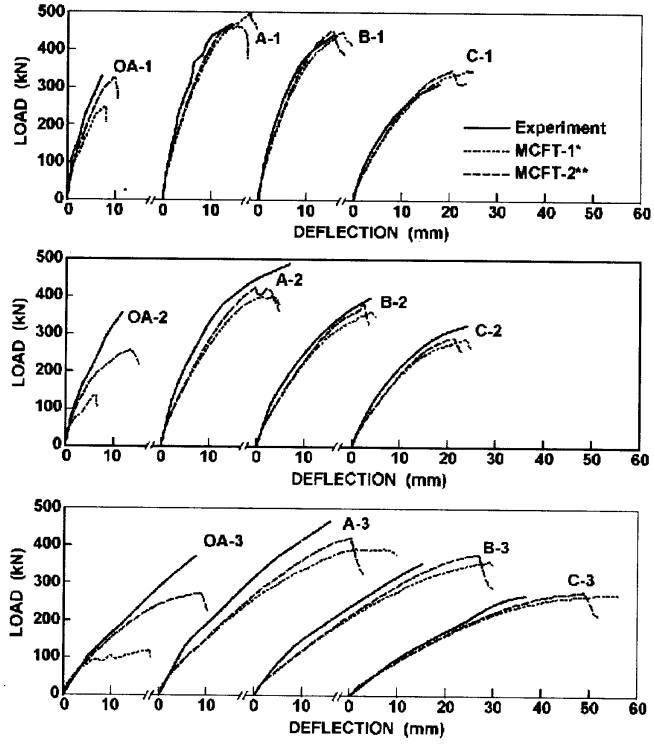

*Without crack width check and residual tension
**With crack width check and residual tension

Fig. 6—Comparison of computed and measured load-deflection responses for Bresler-Scordelis beams.

such as to be critical in shear, being heavily reinforced for flexure and containing light amounts of shear reinforcement. The shear reinforcement ratios ranged from 0.0 to 0.2%. The beams were simply supported and subjected to a concentrated midspan load, producing a shear span-depth ratio ranging from 3.3 to 5.8. Relevant details are provided in Table 1. The effective depth of the bottom longitudinal reinforcement d was 457 mm for all beams. The yield strength of the No. 9 bottom bars was 555 MPa, and of the No. 2 stirrups was 326 MPa.

The series of 12 beams was modeled for FE analysis. All reinforcement was modeled as smeared, with the longitudinal bars smeared within a narrow band of elements coincident with the effective depth of the reinforcement. For analysis purposes, the cracking strength was estimated as $0.33\sqrt{f'_c}$ and the modulus of elasticity was estimated as $5500\sqrt{f'_c}$. A typical FE mesh is shown in Fig. 5. Analyses were performed using both the original MCFT formulations (MCFT-1), and those incorporating the crack width limit and residual tension limit criteria (MCFT-2). For the latter, a conservative value of $0.10 f'_t$ was used.

Shown in Fig. 6 are the computed load-displacement response for the 12 beams. Most of the beams were found to fail in web shear or flexural shear modes. When using the crack width limit and the residual tension, the load-deflection responses are simulated reasonably well. The ratio of the observed-to-predicted ultimate load for the beams has a mean of 1.07 and a coefficient of variation (COV) of 11.1% (refer toTable 2(a)). For the deflection at maximum load, the ratio of predicted to observed values has a mean of 0.90 and a COV of 14.9% (refer to Table 2(b)). These numbers are somewhat more scattered than one normally would like or typically see when applying smeared crack analysis methods to reinforced concrete structures. The intrinsic scatter associated with mechanisms heavily dependent on concrete tensile strength, however, cannot be overlooked.

Table 1—Details of Bresler-Scordelis beams

Beam	$b \times h$, mm	Span, mm	f'_c, MPa	Bottom reinforcement	Top reinforcement	Stirrups	ρ_v %	a/d
OA-1	305 x 552	3660	22.6	4 No. 9	—	—	0.00	3.32
OA-2	305 x 552	4570	23.7	5 No. 9	—	—	0.00	4.14
OA-3	305 x 552	6400	37.6	6 No. 9	—	—	0.00	5.80
A-1	305 x 552	3660	24.1	4 No. 9	2 No.4	No. 2 at 210	0.10	3.32
A-2	305 x 552	4570	24.3	5 No. 9	2 No. 4	No. 2 at 210	0.10	4.14
A-3	305 x 552	6400	35.1	6 No. 9	2 No. 4	No. 2 at 210	0.10	5.80
B-1	229 x 552	3660	24.8	4 No. 9	2 No. 4	No. 2 at 190	0.15	3.32
B-2	229 x 552	4570	23.2	4 No. 9	2 No. 4	No. 2 at 190	0.15	4.14
B-3	229 x 552	6400	38.8	5 No. 9	2 No. 4	No. 2 at 190	0.15	5.80
C-1	152 x 552	3660	29.6	2 No. 9	2 No. 4	No. 2 at 210	0.20	3.32
C-2	152 x 552	4570	23.8	4 No. 9	2 No. 4	No. 2 at 210	0.20	4.14
C-3	152 x 552	6400	35.1	4 No. 9	2 No. 4	No. 2 at 210	0.20	5.80

Table 2(a)—Analysis results for Bresler-Scordelis beams, ultimate load

Beam	$P_{u\text{-}exp}$, kN	$P_{u\text{-}theor}$, kN	$P_{u\text{-}exp}/P_{u\text{-}theor}$
OA-1	334	331	1.01
OA-2	356	292	1.22
OA-3	378	293	1.29
A-1	467	467	1.00
A-2	489	423	1.16
A-3	467	414	1.13
B-1	445	450	0.99
B-2	400	370	1.08
B-3	356	378	0.94
C-1	311	346	0.90
C-2	325	290	1.12
C-3	269	278	0.97
			Mean: 1.07
			COV: 11.1%

Table 2(b)—Analysis results for Bresler-Scordelis beams, displacement at ultimate load

Beam	$\delta_{u\text{-}exp}$, mm	$\delta_{u\text{-}theor}$, mm	$\delta_{u\text{-}exp}/\delta_{u\text{-}theor}$
OA-1	6.6	9.0	0.73
OA-2	11.7	13.5	0.87
OA-3	27.9	31.5	0.89
A-1	14.2	13.5	1.05
A-2	22.9	19.0	1.21
A-3	35.8	38.0	0.94
B-1	13.7	15.0	0.91
B-2	20.8	22.5	0.92
B-3	35.3	47.0	0.75
C-1	17.8	20.5	0.87
C-2	20.1	21.0	0.96
C-3	36.8	49.0	0.75
			Mean: 0.90
			COV: 14.9%

Also shown in Fig. 6 are the load-displacement responses computed using the MCFT formulations without the crack width limit and with no postcracking tensile stress in unreinforced elements. The correlations are inferior, particularly for the beams containing no shear reinforcement where strengths are grossly underestimated. Herein, failure initiates soon after first cracking. Neglecting the crack width check and the residual tension, the ratio of the experimental to computed strength for these beams deteriorates to a mean of 1.38 and a COV of 52.8%. The corresponding experimental to computed deflections at ultimate have a mean of 0.98 and a COV of 39.3%. Thus, the two limits added to the formulation result in a significant improvement in accuracy in computing strength.

The strength of the beams containing no shear reinforcement is extremely sensitive to the level of tension stress permitted in the concrete; hence, by inference, are heavily dependent on mechanisms such as aggregate interlock, tension softening and tension stiffening. Shown in Fig. 7(a) are the responses for Beam OA-1, as obtained using varying amounts of residual tension. The predicted strength is increased from 248 kN, when no residual tension is assumed, to over 400 kN, when $0.2 f'_t$ is assumed. (Consider that f'_t, calculated from $0.33\sqrt{f'_c}$, is a conservative lower bound on the actual cracking stress as determined from prism tests or split cylinder tests.) Similar sensitivities were observed with OA-2 and OA-3. The influence of the residual tension dissipates quickly as shear reinforcement is provided. Shown in Fig. 7(b) are the predicted responses for Beam A-1, containing a nominal 0.1% shear reinforcement. The observed influence on the strength and ductility is significantly less. With regards to maximizing the accuracy of the correlation between the observed and predicted strengths, the optimal value for the residual tension is approximately $0.15 f'_t$; however, $0.10 f'_t$ was chosen because it provides a conservative (safe) prediction in all cases examined herein.

The influence of the crack width limit is more difficult to observe in this particular series of tests. Generally, it works to guard against overestimating the ductility of beams experiencing high levels of web shear strains. Consider Beam A-3 as an example. With the crack width limit in place, the maximum load is achieved at a deflection of 40 mm and drops off fairly abruptly thereafter. This relatively brittle behavior is consistent with the observed response. Without the crack limit, the maximum strength is developed at approximately 48 mm deflection, and the response remains fairly ductile without as rapid a drop off in load.

A second series of specimens examined was that tested by Collins and Stanik.[18] These beams differed from the Bresler and Scordelis beams in two important aspects: 1) the beam sections were much larger, some up to 1000 x 1000 mm in cross section dimension; and 2) the shear span-to-depth ratios (a/d) were lower at approximately 2.7. With the larger cross sections, size- and crack-related mechanisms figure more prominently in the beam response; concrete postcracking tensile stresses, aggregate interlock, and crack shear slip are influenced by the proportionally larger crack widths and greater crack spacings. With the lower shear-span ratios, the influence

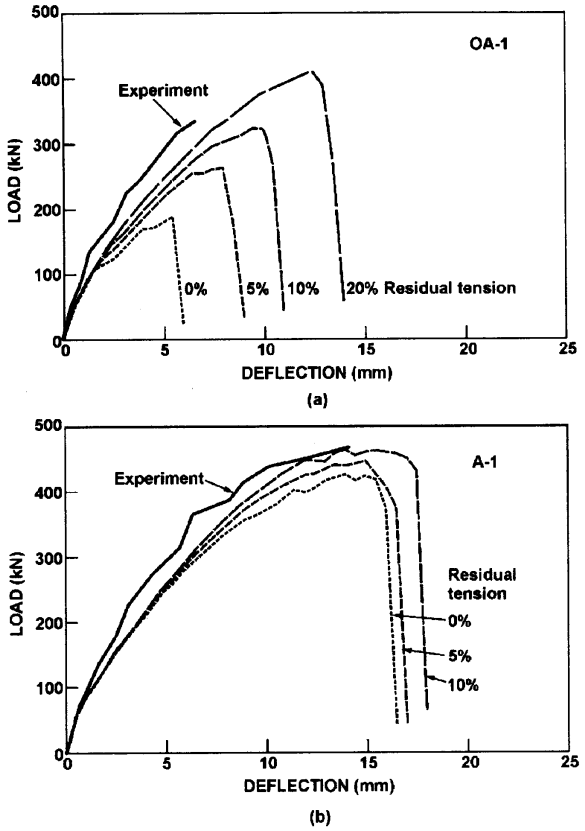

Fig. 7—Sensitivity to residual tension term: (a) Beam OA-1; and (b) Beam A-1.

of direct strut action into the supports becomes more significant, and the ability of cracks to undergo rotation is tested. Ten of the larger beams were selected for analysis; some relevant details are provided in Table 3. Note the exceptionally low values of shear reinforcement. Each of these beams experienced a shear-related failure mode.

The Collins-Stanik beams were modeled in the same manner as the Bresler-Scordelis beams. All reinforcement was modeled as smeared. The crack width limit of 2.0 mm, and a residual tension of $0.10 f'_c$ were typically used. The results obtained, as with the unreinforced Bresler-Scordelis beams, demonstrated some scatter but were reasonably accurate. Shown in Fig. 8, for example, is the correlation obtained for the observed and calculated load-deflection responses of Beam WM100D, one of the least well-predicted beams. Stiffness and strength are overestimated, but the brittle failure mode is adequately captured. Given in Table 4 are the predicted and measured strengths of all 10 beams examined. The ratio of the experimental to theoretical shear strength has a mean of 0.93 and a COV of 13.9%, an acceptable degree of accuracy. In these beams, a significant degree of slip was measured along the crack surfaces. This slip may have retarded the reorientation of crack directions and principal stresses, as assumed in the MCFT, preventing the formation of a pronounced strut action into the supports. Note also that the analyses systematically overestimated the strengths of beams containing distributed longitudinal reinforcement (i.e., beams with the designation "D"). The crack control effectiveness of the distributed reinforcement is not as pronounced as inherently assumed in the analysis, derived from increased tension stiffening due to the smeared reinforcement modeling.

SECTIONAL ANALYSES

Beam section analysis procedures have been used by various researchers to model beams in shear. One such procedure was described in Reference 20; it uses a layered section algorithm

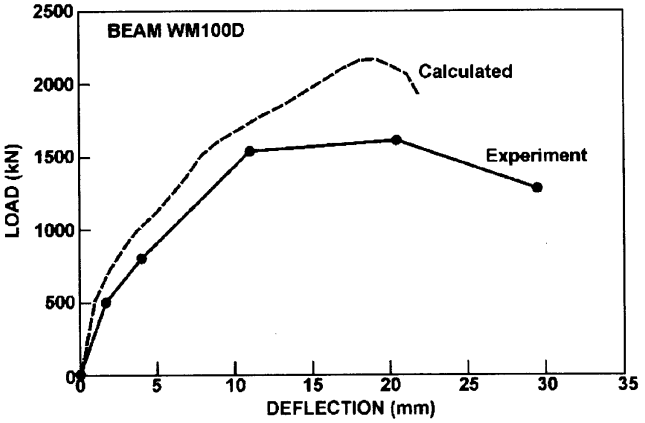

Fig. 8—Measured and calculated load-deflection response for Beam WM100D.

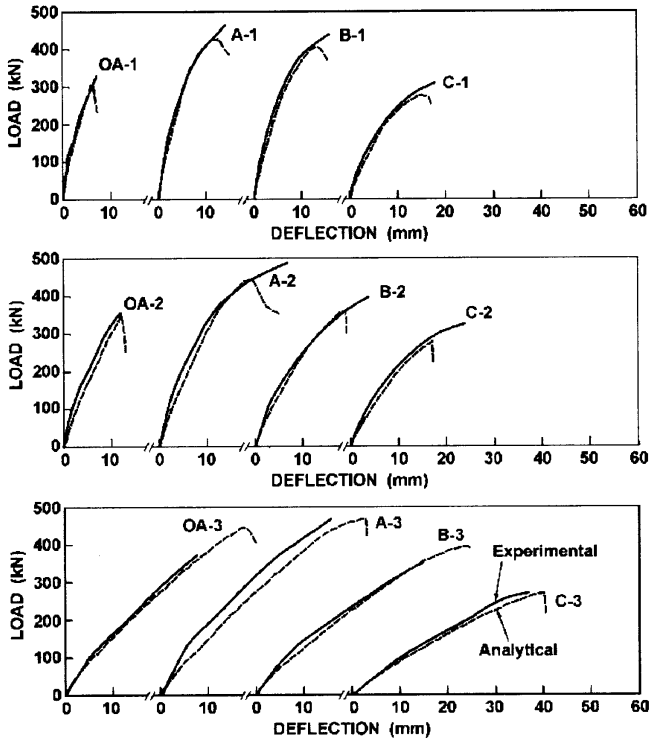

Fig. 9—Comparison of results of frame analyses for Bresler-Scordelis beams.

in which a beam section is discretized into a number of concrete layers and reinforcement components. Each concrete layer is analyzed for two-dimensional strain conditions within the plane of the beam according to the equilibrium, compatibility, and constitutive response requirements of the MCFT. Analyzing two sections within close proximity provides a means of determining the shear flow distribution through the depth of the cross section. Alternatively, a more approximate (and much quicker) analysis can be undertaken by assuming a constant shear strain distribution through the depth of the section. The constant shear strain assumption provides accurate approximations in most cases. Analyses of several sets of beams critical in shear are reported in Reference 20, showing good correlation to test results. Most of these beams, however, were well reinforced in shear.

A nonlinear frame analysis algorithm was also developed, incorporating the sectional procedures previously described, together with the constant shear strain assumption. Analyses of large-scale two-story frame specimens[21,22] that sustained shear-related failures showed good correlation. These frames,

Table 3—Details of Collins-Stanik beams

Beam	b x h	Span, mm	f'_c, MPa	A_s lbd, %	Stirrups	ρ_v, %	a/d
WM100D	1000 x 1000	2700	38	1.40	No. 3 at 375	0.038	2.70
WM100C	1000 x 1000	2700	41	1.40	No. 3 at 375	0.038	2.70
BM100D	300 x 1000	2700	46	1.05	No. 3 at 600	0.079	2.70
BM100	300 x 1000	2700	46	0.76	No. 3 at 600	0.079	2.70
BN100D	300 x 1000	2700	37	1.05	—	0.000	2.70
BN100	300 x 1000	2700	37	0.76	—	0.000	2.70
UM100D	300 x 1000	2700	42	1.05	No. 3 at 600	0.079	2.70
UM100	300 x 1000	2700	42	0.76	No. 3 at 600	0.079	2.70
UN100D	300 x 1000	2700	43	1.05	—	0.000	2.70
UN100	300 x 1000	2700	43	0.76	—	0.000	2.70

Table 4—Analysis results for Collins-Stanik beams

Beam	$V_{u\text{-}exp}$, kN	$V_{u\text{-}theor}$, kN	$V_{u\text{-}exp}/V_{u\text{-}theor}$
WM100D	834	1057	0.79
WM100C	699	680	1.03
BM100D	462	514	0.90
BM100	343	366	0.94
BN100D	258	382	0.68
BN100	192	188	1.02
UM100D	910	924	0.98
UM100	750	698	1.07
UN100D	637	756	0.84
UN100	593	552	1.07
			Mean: 0.93
			COV: 13.9%

Table 5—Frame analysis results for Bresler-Scordelis beams

Beam	$V_{u\text{-}exp}$, kN	$V_{u\text{-}theor}$, kN	$V_{u\text{-}exp}/V_{u\text{-}theor}$
OA_1	167	151	1.11
OA-2	178	173	1.03
OA-3	189	222	0.85
A-1	234	213	1.10
A-2	245	222	1.10
A-3	234	232	1.01
B-1	221	203	1.09
B-2	200	179	1.12
B-3	175	195	0.90
C-1	156	137	1.13
C-2	162	138	1.18
C-3	135	134	1.01
			Mean: 1.05
			COV: 9.3%

however, also contained adequate amounts of shear reinforcement (approximately 0.5%).

To gage the accuracy of the sectional procedures for shear-critical beams containing little or no shear reinforcement, the frame analysis algorithm was used in modeling the Bresler-Scordelis beams. Frame models composed of 10 equal-length beam segments were used to model the half-span of each beam. All section details and material properties were as previously described. The crack width limit and the residual tension provision are currently not installed in the frame analysis algorithm; the need is not as great because all forces must be resisted by sectional equilibrium without the benefit of strut action to the supports. Further, the crack width check has no relevance in the context of a sectional analysis procedure, and the concrete tensile stress calculations are not limited by the mesh configuration.

Shown in Fig. 9 are comparisons of the measured and computed deflection responses for the 12 beams. Given in Table 5 is the correlation obtained for the beam shear strengths. The strength, stiffness, and ductility of the beams are modeled well, with an accuracy comparable to that of the nonlinear FE analyses (NLFEA)(but requiring considerably less computational effort). The ratio of experimental-to-calculated shear strength has a mean of 1.05 and a COV of only 9.3%. Failure mode, reinforcement strains, and other measure of sectional response were also modeled well. Note that the beams containing no shear reinforcement (OA-1, OA-2, OA-3) were modeled with better accuracy than obtained with the NLFEA. In the sectional analyses, tension stiffening is permitted in any concrete layer within 7-1/2 bar diameters of a longitudinal bar, subject to limits imposed by reinforcing bar yielding. Thus, the concrete tension is handled in a more rational manner than done so in the FE formulation, where the residual tension is an arbitrary compensation for incomplete modeling.

CONCLUSIONS

Smeared, rotating crack models can provide a viable and accurate method for analysis for shear-critical concrete beams containing little or no shear reinforcement. In particular, the formulations of the modified compression field theory remain valid provided that two minor limits are imposed on the original constitutive relations, one relating to tensile stresses in the concrete and the other to crack widths. More specifically:

1. Postcracking tensile stresses are required in unreinforced or lightly reinforced concrete elements representing the web of a shear-critical beam, for a viable internal load resisting mechanism to form. This tension, in reality, takes its origin from a tension stiffening mechanism associated with the nearby longitudinal reinforcement, and from aggregate and tension softening mechanisms. A conservative value for the lower limit on this residual tension can be taken as $0.10 f'_t$; and

2. Shear slip along the surfaces of wide cracks can result in a divergence between the directions of principal stress and the apparent directions of principal strain. An overestimation of the reorientation of the stress trajectories and hence in the ductility of the beam may result. To guard against this, the principal compressive stress is rapidly diminished in elements containing cracks exceeding a limit of 2.0 mm in width.

With the addition of these two limits, the original MCFT formulation provides a viable analysis model for NLFEA of shear-critical beams while retaining the assumption of coaxiality of principal stresses and strains. For beams containing shear rein-

forcement ratios exceeding the nominally low value of ρ_v = 0.10%, correlation with experimental results is excellent. Failure mode, postcracking stiffness, ultimate strength, and ductility are accurately simulated. For beams containing no shear reinforcement, the accuracy is reduced but still acceptable, giving the natural scatter associated with mechanisms lightly dependent on concrete tensile strength.

Sectional analysis procedures, based on the MCFT, were also shown to provide good results. A nonlinear frame analysis procedure, incorporating a layered section algorithm and assuming a constant shear strain through the section, gives results comparable in accuracy to the FE analyses.

To improve the performance of smeared crack models to this type of analyses, additional developmental work is required in two respects:

1. An improved model is required for postcracking tension in the unreinforced elements, better quantifying the influences of tension stiffening effects from nearby reinforcement and from aggregate interlock and tension softening. This will eliminate the need for a constant value residual tension limit; and

2. Allowance should be made in the compatibility relations for discrete shear slip along the crack surfaces. This will permit the rotation of the principal stresses to lag behind the apparent rotation of the principals strains. In turn, this will result in less reorientation of the stress fields and less ductility in the computed responses. Such a formulation will likely eliminate the need for a crack width limit.

Work in these two areas is progressing.

ACKNOWLEDGMENTS

Thanks are extended to the following contributors: Filippo Bucci for analysis of the Collins/Stanik beams; Alex Cheng for finite element analysis of the Bresler-Scordelis beams; and Boa Tien Chen for frame modeling of the Bresler-Scordelis beams. Thanks also to Michael Collins for access to the data from his beam tests.

NOTATIONS

a	=	aggregate size, mm
a/d	=	shear span-to-depth ratio
A_s	=	area of longitudinal reinforcement
b	=	width of beam section
d	=	effective depth to longitudinal reinforcement
f'_c	=	compressive strength of concrete (cylinder)
f_p	=	peak compressive stress in cracked concrete
f_s	=	average stress in reinforcement component
f'_t	=	tensile strength of concrete
f_y	=	yield stress of reinforcement component
f_{c1}	=	principal tensile stress in concrete
f_{c2}	=	principal compressive stress in concrete
h	=	depth of beam section
P_u	=	ultimate load capacity of beam
v_{ci}	=	shear stress on crack surface
v_{cimax}	=	maximum shear stress that can be resisted on crack surface
V_u	=	ultimate shear force on beam
w	=	crack width, mm
β	=	shear retention factor
β_d	=	compressive softening factor
ε_1	=	principal tensile strain in concrete
ε_2	=	principal compressive strain in concrete
ε_o	=	cylinder strain at peak compressive stress, f'_c
ε_p	=	concrete strain at peak compressive stress, f_p
θ_{ni}	=	angle between reinforcement and normal to crack
ρ_i	=	reinforcement ratio for i-th reinforcement component
ρ_v	=	shear reinforcement ratio

REFERENCES

1. Vecchio, F. J., and Collins, M. P., "Modified Compression Field Theory for Reinforced Concrete Elements Subjected to Shear," ACI JOURNAL, *Proceedings* V. 83, No. 2, Mar.-Apr. 1986, pp. 219-231.

2. Collins, M. P.; Mitchell, D.; Adebar, P.; and Vecchio, F. J., "General Shear Design Method," *ACI Structural Journal*, V. 93, No. 1, Jan.-Feb. 1996, pp. 36-45.

3. Vecchio, F. J., "Reinforced Concrete Membrane Element Formulations," *ASCE Journal of Structural Engineering*, V. 116, No. 3, Mar. 1990, pp. 730-750.

4. Vecchio, F. J., and Selby, R. G., "Towards Compression-Field Analysis of Reinforced Concrete Solids," *ASCE Journal of Structural Engineering*, V. 117, No. 6, June 1991, pp. 1740-1758.

5. Polak, M. A., and Vecchio, F. J., "Nonlinear Analysis of Reinforced Concrete Shells," *ASCE Journal of Structural Engineering*, V. 119, No. 12, Dec. 1993, pp. 3439-3462.

6. Vecchio, F. J.; Polak, M. A.; and Selby, R. G., "Nonlinear Analysis of Reinforced Concrete: The University of Toronto Experience," *Proceedings*, Third Asian-Pacific Conference on Computational Mechanics, Seoul, Korea, Sept. 1996.

7. Hsu, T. T. C., "Nonlinear Analysis of Concrete Membrane Elements," *ACI Structural Journal*, V. 88, No. 5, Sept.-Oct. 1991, pp. 552-561.

8. Ayoub, A., and Filippou, F. C., "Nonlinear Finite Element Analysis of Reinforced Concrete Shear Panels and Walls," *ASCE Journal of Structural Engineering*, V. 124, No. 3, Mar. 1998, pp. 298-308.

9. Foster, S. J., "The Structural Behavior of Reinforced Concrete Deep Beams," PhD thesis, University of New South Wales, Australia, 1992.

10. Okamura, H., and Maekawa, K., "Nonlinear Analysis and Constitutive Models of Reinforced Concrete," University of Tokyo, *Publication* ISBN-7655-1506-0, 1991, pp. 182.

11. Kaufmann, W., and Marti, P., "Structural Concrete: Cracked Membrane Model," *ASCE Journal of Structural Engineering*, V. 124, No. 12, Dec. 1998, 1467-1475.

12. Chung, W., and Ahmad, S. H., "Analytical Model for Shear Critical Reinforced Concrete Members," *ASCE Journal of Structural Engineering*, V. 121, No. 6, June 1995, pp. 1023-1030.

13. Vecchio, F. J., and Collins, M. P., "Analytical Model for Shear Critical Reinforced Concrete Members," Discussion, *ASCE Journal of Structural Engineering*, V. 122, No. 9, Sept. 1996, pp. 1123-1124.

14. Hsu, T. T. C., and Zhang, L. X., "Nonlinear Analysis of Membrane Elements by Fixed-Angle Softened-Truss Model," *ACI Structural Journal*, V. 94, No. 5, Sept.-Oct. 1997, pp. 483-492.

15. Vecchio, F. J., "Nonlinear Finite Element Analysis of Reinforced Concrete Membranes," *ACI Structural Journal*, V. 86, No. 1, Jan.-Feb. 1989, pp. 26-35.

16. Vecchio, F. J., and Collins, M. P., "Compression Response of Cracked Reinforced Concrete," *ASCE Journal of Structural Engineering*, V. 119, No. 12, Dec. 1993, pp. 3590-3610.

17. Walraven, J., "Fundamental Analysis of Aggregate Interlock," *Journal of Structural Engineering*, ASCE, V. 107, No. 11, 1981, pp. 2245-2270.

18. Stanik, B. A., "The Influence of Concrete Strength, Distribution of Longitudinal Reinforcement, Amount of Transverse Reinforcement, and Member Size on Shear Strength of Reinforced Concrete Members," MASc thesis, University of Toronto, 1998, 711 pp.

19. Bresler, B., and Scordelis, A. C., "Shear Strength of Reinforced Concrete Beams," ACI JOURNAL, *Proceedings* V. 60, No. 1, Jan.-Feb. 1963, pp. 51-74.

20. Vecchio, F. J., and Collins, M. P., "Predicting the Response of Reinforced Concrete Beams Subjected to Shear Using the Modified Compression Field Theory," *ACI Structural Journal*, V. 85, No. 3, May-June 1988, pp. 258-268.

21. Vecchio, F. J., and Emara, M. B., "Shear Deformations in Reinforced Concrete Frames," *ACI Structural Journal*, V. 89, No. 1, Jan.-Feb. 1992, pp. 45-56.

22. Vecchio, F. J., and Balopoulou, S., "On the Nonlinear Behaviour of Reinforced Concrete Frames," *Canadian Journal of Civil Engineering*, V. 17, No. 5, 1990, pp. 698-704.